

UDC 53.072; 53:681.3

A.A. Kupchishin<sup>1</sup>, A.I. Kupchishin<sup>2</sup>, E.V. Shmygalev<sup>1\*</sup>, T.A. Shmygaleva<sup>1\*</sup>, Sh.E. Jeleunova<sup>1</sup><sup>1</sup>Al-Farabi Kazakh National University, Kazakhstan, Almaty<sup>2</sup>Kazak National Pedagogical University named after Abai, Kazakhstan, Almaty

\*E-mail: Shmyg1953@mail.ru

**Mathematical modeling of radiating defects in iron**

**Abstract.** Processes of radiation formation of defects in the iron exposed to radiation by various ions are considered in the work. The algorithm is developed for calculation of cascadelly - probabilistic functions, concentration of radiation defects, computations are lead, the regularities arising at calculations of cascadelly - probabilistic functions depending on number of interactions and depth of penetration of particles, concentration of radiation defects are revealed by an ionic irradiation in iron. Results of calculations are presented in the form of tables and schedules.

**Keywords:** modeling, defects, iron, ions, steel, cast iron.

**Introduction**

Alloys on the basis of iron (steel, cast iron) are considered in the work, as now beams of ions are intensively applied in mechanical engineering at deriving of ultrastrong details and materials. The cascadelly - probabilistic method (CPM) is used for this purpose, in which basis is recipience of

analytical expressions and further use of cascadelly – probabilistic functions (CPF). CPF mean probabilities that the particle generated on some depth  $h'$  will reach of depth  $h$  after  $n$  numbers impacts.

**Experiment**

CPF expression for ions in view of losses of energy has a following appearance [1]:

$$\psi_n(h', h, E_0) = \frac{1}{n! \lambda_0^n} \left( \frac{E_0 - kh'}{E_0 - kh} \right)^{-l} \exp\left(\frac{h - h'}{\lambda_0}\right) * \left[ \frac{\ln\left(\frac{E_0 - kh'}{E_0 - kh}\right)}{ak} - (h - h') \right]^n. \quad (1)$$

For calculation CPF the following modernized formula convenient for computation is received:

$$\psi_n(h', h, E_0) = \prod_{i=1}^n \left[ \left( \frac{\ln\left(\frac{E_0 - kh'}{E_0 - kh}\right)}{ak} - (h - h') \right) \frac{1}{\lambda_0^i} \right] * \exp\left(\frac{h - h'}{\lambda_0} - \frac{1}{\lambda_0 ak} \left( \frac{E_0 - kh'}{E_0 - kh} \right)\right) \quad (2)$$

where  $n$  is the number of interactions,  $h'$ ,  $h$  are depths of generation and registration of an ion accordingly,  $l_0$ ,  $a$ ,  $E_0$ ,  $k$  are parameters of approximation.

To find parameters of approximation was used the following approximation expression [1]:

$$\sigma(h) = \sigma_0 \left( \frac{1}{a(E_0 - kh)} - 1 \right) \quad (3)$$

Dependences approximation curve  $s$  from  $h$  are resulted in figure 1.

Further calculations of cascadelly - probabilistic functions depending on number of interactions and depth of penetration of particles are lead. Areas of a finding of result are found and the regularities of CPF behaviour from number of interactions and from depth of penetration of particles are revealed (tables 1, 2, figures. 2, 3).

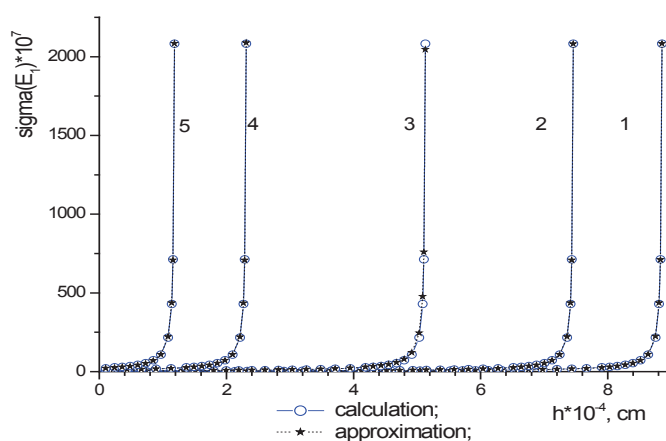


**Figure 1** – Approximation of the modified section of cascadelly - probabilistic function: for nitrogen in iron for  $E_0 = 1000$  (1), 800 (2), 500 (3), 200 (4), 100 (5) keV. Coefficient of correlation  $\eta = 0,9999$ .

**Table 1** – Dependence of displacement percent of the left and right borders of result area from number of interactions for silicon in iron for a)  $E_0 = 1000$  keV; b)  $E_0 = 800$  keV c)  $E_0 = 500$  keV d)  $E_0 = 200$  keV e)  $E_0 = 100$  keV

| $h \cdot 10^4, \text{ sm}$ | $B_1, \%$ | $B_2, \%$ | $N_n$ | $B_3, \%$ |
|----------------------------|-----------|-----------|-------|-----------|
| 0,5                        | 35        | 23        | 20    | 58        |
| 1,2                        | 34        | -3        | 35    | 31        |
| 1,9                        | 38        | -18       | 45    | 20        |
| 2,6                        | 44        | -31       | 55    | 13        |
| 3,3                        | 50,8      | -41       | 69    | 9,8       |
| 4                          | 58,3      | -51,7     | 82    | 6,6       |
| 4,7                        | 67,3      | -63,2     | 105   | 4,1       |
| 5,4                        | 79,1      | -77,1     | 130   | 2         |

a)

| $h \cdot 10^4, \text{ sm}$ | $B_1, \%$ | $B_2, \%$ | $N_n$ | $B_3, \%$ |
|----------------------------|-----------|-----------|-------|-----------|
| 0,5                        | 32        | 16        | 22    | 48        |
| 1,1                        | 32,5      | -6        | 35    | 26,5      |
| 1,7                        | 37,5      | -19,5     | 50    | 28        |
| 2,3                        | 44,2      | -32       | 62    | 12,2      |
| 2,9                        | 51,6      | -43,5     | 70    | 8,1       |
| 3,5                        | 60,2      | -54,6     | 79    | 5,6       |
| 4,1                        | 70,8      | -67,5     | 100   | 3,3       |
| 4,7                        | 86,15     | -85,05    | 140   | 1,1       |

b)

| $h \cdot 10^4, \text{ sm}$ | $B_1, \%$ | $B_2, \%$ | $N_n$ | $B_3, \%$ |
|----------------------------|-----------|-----------|-------|-----------|
| 0,1                        | 42        | 47        | 13    | 89        |
| 0,5                        | 28        | 58        | 33    | 86        |
| 0,9                        | 32        | -11       | 48    | 21        |
| 1,3                        | 38        | -24       | 60    | 14        |
| 1,7                        | 45,5      | -35,5     | 70    | 10        |
| 2,1                        | 54        | -47       | 85    | 7         |
| 2,5                        | 64,3      | -60,2     | 99    | 4,1       |
| 2,9                        | 78,15     | -76,2     | 125   | 1,95      |

c)

Continuation of the table 3

| $h \cdot 10^4, \text{ sm}$ | $B_1, \%$ | $B_2, \%$ | $N_n$ | $B_3, \%$ |
|----------------------------|-----------|-----------|-------|-----------|
| 0,1                        | 27        | 21        | 25    | 48        |
| 0,3                        | 26,5      | -3,5      | 46    | 23        |
| 0,5                        | 33,5      | -19       | 62    | 14,5      |
| 0,7                        | 43        | -33,5     | 74    | 9,5       |
| 0,9                        | 54,7      | -49       | 91    | 5,7       |
| 1,1                        | 70,5      | -67,6     | 120   | 2,9       |

d)

| $h \cdot 10^4, \text{ sm}$ | $B_1, \%$ | $B_2, \%$ | $N_n$ | $B_3, \%$ |
|----------------------------|-----------|-----------|-------|-----------|
| 0,1                        | 48        | 60        | 12    | 108       |
| 0,8                        | 23,5      | 10        | 32    | 33,5      |
| 1,5                        | 25        | -4        | 45    | 21        |
| 2,2                        | 29,7      | -14,5     | 60    | 15,2      |
| 2,9                        | 36        | -25       | 72    | 11        |
| 3,6                        | 43,5      | -35,4     | 80    | 8,1       |
| 4,3                        | 52,5      | -46,5     | 95    | 6         |
| 5                          | 63,4      | -59,6     | 110   | 3,8       |
| 5,7                        | 78,05     | -76,3     | 135   | 1,75      |

e)

**Table 2** – Dependence of displacement percent of the left and right borders of result area from depth of penetration for silicon in iron for a)  $E_0=1000$  keV; b)  $E_0=800$  keV; c)  $E_0=500$  keV; d)  $E_0=200$  keV; e)  $E_0=100$  keV

| $h \cdot 10^4, \text{ sm}$ | $h/\lambda$ | $C_1, \%$ | $C_2, \%$ | $N_h$ | $C_3, \%$ |
|----------------------------|-------------|-----------|-----------|-------|-----------|
| 0,5                        | 473         | 17,5      | 41,2      | 22    | 58,7      |
| 1,2                        | 1477        | -4,2      | 34        | 49    | 29,8      |
| 1,9                        | 3062        | -17       | 36,3      | 90    | 19,3      |
| 2,6                        | 5585        | -25,5     | 37,5      | 155   | 12        |
| 3,3                        | 9765        | -30,3     | 37        | 285   | 6,7       |
| 4                          | 17310       | -30,65    | 33,7      | 625   | 3,05      |
| 4,7                        | 33513       | -24,65    | 25,35     | 2550  | 0,7       |

a)

| $h \cdot 10^4, \text{ sm}$ | $h/\lambda$ | $C_1, \%$ | $C_2, \%$ | $N_h$ | $C_3, \%$ |
|----------------------------|-------------|-----------|-----------|-------|-----------|
| 0,5                        | 670         | 13        | 35        | 25    | 48        |
| 1,1                        | 1899        | -6,5      | 33,7      | 62    | 27,2      |
| 1,7                        | 3832        | -18,5     | 34,7      | 112   | 16,2      |
| 2,3                        | 6943        | -26,5     | 36,5      | 200   | 10        |
| 2,9                        | 12255       | -30,5     | 36        | 355   | 5,5       |
| 3,5                        | 22464       | -29,22    | 31,3      | 915   | 2,08      |
| 4,1                        | 47689       | -20,115   | 20,36     | 6700  | 0,145     |

b)

| $h \cdot 10^4, \text{ sm}$ | $h/\lambda$ | $C_1, \%$ | $C_2, \%$ | $N_h$ | $C_3, \%$ |
|----------------------------|-------------|-----------|-----------|-------|-----------|
| 0,1                        | 215         | 35        | 57        | 12    | 94        |
| 0,5                        | 1343        | 3,5       | 31        | 44    | 34,5      |
| 0,9                        | 3056        | -11       | 31,5      | 85    | 20,5      |
| 1,3                        | 5719        | -21,3     | 34        | 138   | 12,7      |
| 1,7                        | 10075       | -28       | 35,5      | 250   | 7,5       |
| 2,1                        | 17919       | -30,1     | 33,5      | 585   | 3,4       |
| 2,5                        | 34964       | -24,95    | 25,77     | 2250  | 0,82      |

c)

Continuation of the table 2

| $h \cdot 10^4, \text{ sm}$ | $h/\lambda$ | $C_{12}, \%$ | $C_{22}, \%$ | $N_h$ | $C_{32}, \%$ |
|----------------------------|-------------|--------------|--------------|-------|--------------|
| 0,1                        | 715         | 16,5         | 30,5         | 25    | 47           |
| 0,3                        | 2714        | -4,5         | 28           | 62    | 23,5         |
| 0,5                        | 5949        | -17,7        | 31,5         | 126   | 13,8         |
| 0,7                        | 11664       | -26,9        | 34,2         | 242   | 7,3          |
| 0,9                        | 23618       | -28,75       | 31,2         | 712   | 2,45         |
| 1,1                        | 60923       | -17,338      | 17,45        | 15500 | 0,112        |

d)

| $h \cdot 10^4, \text{ sm}$ | $h/\lambda$ | $C_{12}, \%$ | $C_{22}, \%$ | $N_h$ | $C_{32}, \%$ |
|----------------------------|-------------|--------------|--------------|-------|--------------|
| 0,1                        | 151         | 43           | 63           | 7     | 106          |
| 0,8                        | 1403        | 7,8          | 26           | 40    | 33,8         |
| 1,5                        | 3088        | -4,5         | 26           | 71    | 21,5         |
| 2,2                        | 5428        | -14          | 29           | 112   | 15           |
| 2,9                        | 8831        | -21,9        | 32           | 190   | 10,1         |
| 3,6                        | 14135       | -27,4        | 33,4         | 310   | 6            |
| 4,3                        | 23362       | -28,65       | 31,3         | 700   | 2,65         |
| 5                          | 42992       | -22,784      | 23,322       | 3550  | 0,538        |

e)

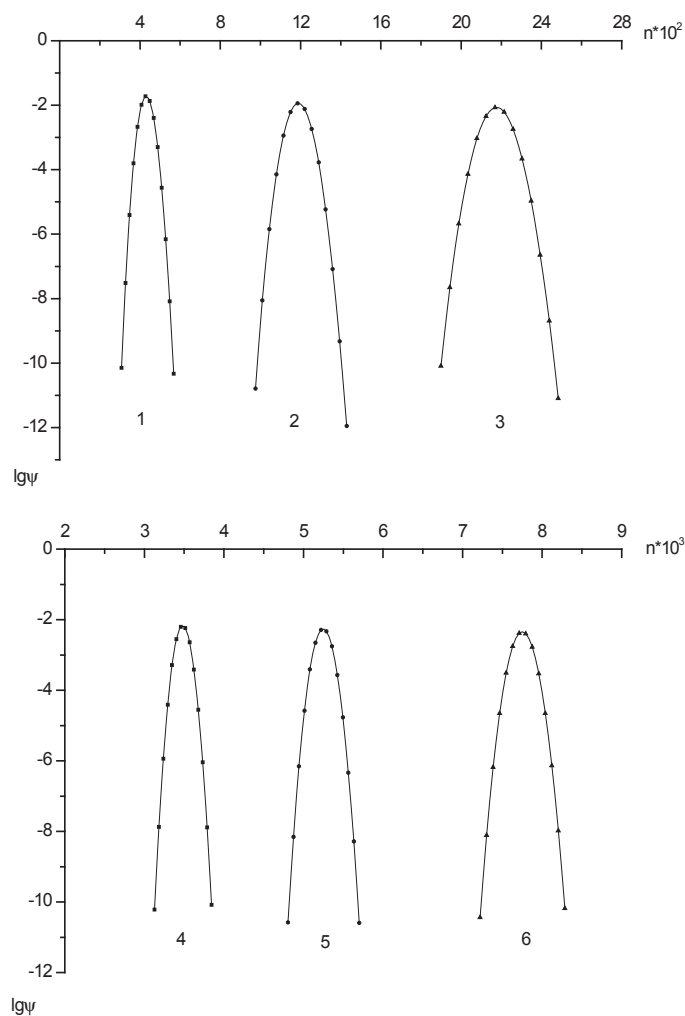


**Figure 2** – CPF dependence for silicon in iron from number of interactions for  $E_0 = 1000 \text{ keV}$  and  $h = 0,5 \cdot 10^{-4}; 1,2 \cdot 10^{-4}; 1,9 \cdot 10^{-4}; 2,6 \cdot 10^{-4}; 3,3 \cdot 10^{-4}; 4,0 \cdot 10^{-4} \text{ (cm)}$  (1-6).

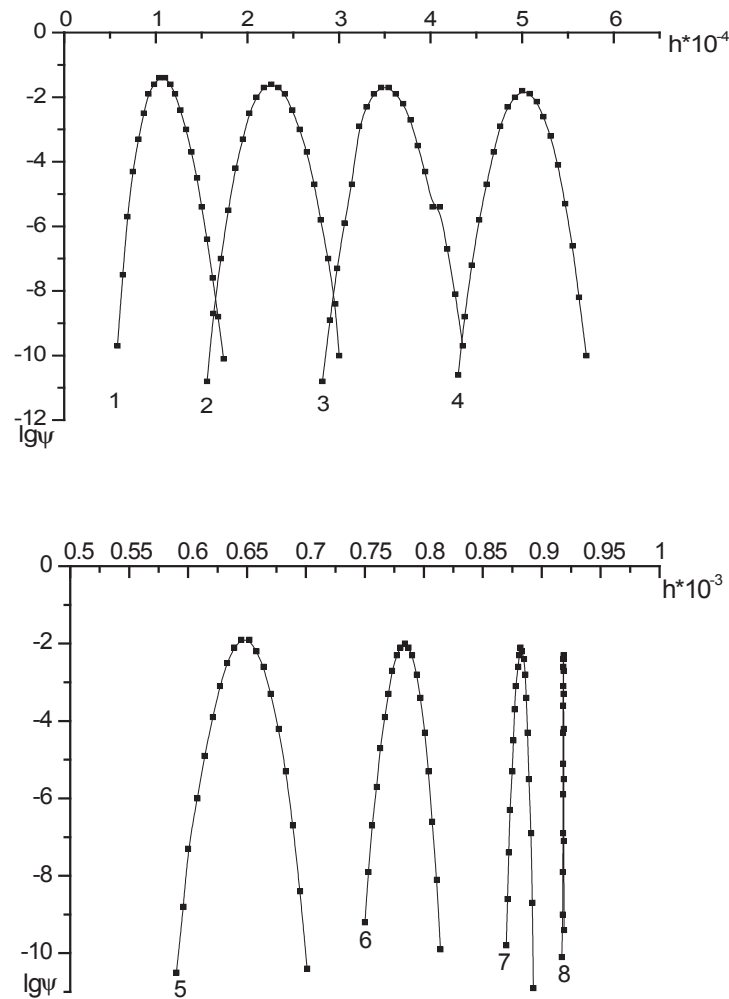


**Figure 3** – CPF dependence for boron in iron from depth of penetration for  $E_0=1000$  keV and  $n = 113; 264; 471; 768; 1217; 1961; 3404; 7301$  (1–8).

## Results and Discussion

Concentration of radiating defects at an ionic irradiation was calculated under the following formula [1].

$$C_k(E_0, h) = \frac{E_d}{E_c} \frac{(E_{2\max} - E_c)}{(E_{2\max} - E_d)} \sum_{n=n_0}^{n_1} \int_{h-k\lambda_2}^h \psi_n(h') \exp\left(-\frac{h-h'}{\lambda_2}\right) \frac{dh'}{\lambda_1(h')\lambda_2} \quad (4)$$

The regularities of concentration behaviour of radiating defects depending on various factors are received. For easy flying particles and easy targets curves increase, peaking, then decrease up to a zero. For  $E_c = 50$  keV in section there is a maximum that speaks about localization of cascade areas on small depth. With an increase of nuclear weight of a flying particle value of function in a point of a maximum increases and, consequently, curves pass

above while values of depths decrease, i.e. the large concentration of vacancies clusters in near-surface area is formed. With an increase of initial energy of a particle area of damage are displaced in depth of a material. At identical  $E_0$  and  $E_c$  for heavier particles on unit of a way of ion movement it is formed more areas. With energy of flying particle  $E_0=100$  KeV a maximum of function is at a surface of a target, and its value is not enough and quickly turn into

zero, very small damaged area which lays within the limits of 10–100 nanometers consequently is formed. Results of calculations are presented in figure 4.

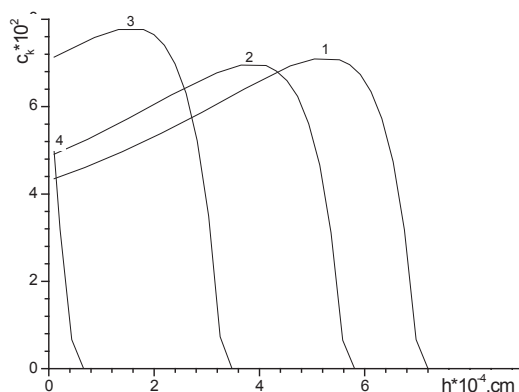


**Figure 4** – Sections of allocations on depth of vacancies clusters at an ionic irradiation for nitrogen in iron for  $E_c=100$  keV,  $E_0=1000$  (1), 800 (2), 500 (3), 200(4) keV.

#### Reference

1 Kupchishin A.I., Kylyshkanov M., Shmygal-eva T.A., etc. Modelling on the PC and experimen-

tal researches of radiating processes in iron and firm alloys. – Almaty: Abay KazNAU, Al-Farabi KazNUSRI of ETP, Open Company “KAMA”, 2010. – P. 263.

А.И. Купчишин, А.А. Купчишин, Т.А. Шмыгалева, Е.В. Шмыгалиев, Ш.Е. Джеллеунова  
**Радиациялық мін теміріндегі математикалық үлгілеу**

Бұл жұмыста әртүрлі ион сәулеге түсірілген темірдегі радиациялық білімінің үдерістері қарастырылған. Мұнда каскадты ықтимал функциялар есептеуінің алгоритмі әзірленді, өзара әрекеттесу саны мен өтімділік тереңдігіне байланысты функция күйіне талдау жасалынды, каскадты ықтимал функциялардың есептеулерінде өзара әрекеттесулерден тұратын сан және бөлшектердің өтімділік тереңдігі, радиациялық міндердің шоғырландыруына байланысты темірдегі иондық сәулеге түсіру кезінде пайда болған заңдылықтар анықталды. Есептеулер қорытындылары графиктер және кестелер түрінде келтірілген.

**Түйін сөздер:** модельдеу, ақаулар, үтік, иондар, алмас, шойын.

А.И. Купчишин, А.А. Купчишин, Т.А. Шмыгалева, Е.В. Шмыгалиев, Ш.Е. Джеллеунова  
**Математическое моделирование радиационных дефектов в железе**

В работе рассмотрены процессы радиационного дефектообразования в железе, облученном различными ионами. Разработан алгоритм для расчета каскадно-вероятностных функций, концентрации радиационных дефектов, проведены расчеты, выявлены закономерности, возникающие при расчетах каскадно-вероятностных функций в зависимости от числа взаимодействий и глубины проникновения частиц, концентрации радиационных дефектов при ионном облучении в железе. Результаты расчетов приведены в виде графиков и таблиц.

**Ключевые слова:** моделирование, дефекты, утюг, ионы, сталь, чугун.